Petrographic and Geochemical Data for Jurassic Basalt from Eight Cores, Newark Basin, New Jersey

Richard P. Tollo[1], David P. Hawkins[2], and David Gottfried[3]

[1]Department of Geology, George Washington University, Washington, DC 20052
[2]Department of Earth and Planetary Sciences, Washington University, St. Louis, MO 63130
[3]U.S. Geological Survey, National Center, Reston, VA 22092

Introduction

The eight cores examined in this study were obtained by the U.S. Army Corps of Engineers as part of an engineering assessment of the bedrock properties along the proposed route of a flood diversion tunnel for the Passaic River in northern New Jersey (Figure 1; see also Fedosh and Smoot, 1988). These cores provide an important partial cross-section through each of the major volcanic units of the early Mesozoic Newark basin and have made possible a detailed and systematic investigation of the stratigraphic compositional variation characterizing each extrusive formation.

This paper contains the detailed petrographic and geochemical data that serve as the basis for the discussions presented in Tollo and Gottfried (in press). Schematic columnar sections are presented to show the physical features observed in each core during logging and sampling. Detailed petrographic data are presented in tabular form for each of the major flow units. Major and trace element data are presented for each sample examined in this study.

Geologic Setting

The Newark basin is a deeply-eroded, half-graben encompassing an area of approximately 50,000 square miles (129,500 km^2) in northern New Jersey, southeastern New York, and eastern Pennsylvania and is part of a series of exposed basins extending discontinuously throughout the eastern Appalachian orogen from South Carolina to Nova Scotia. Within the United States, the Newark basin is one of four major basins containing exposures of early Jurassic basalt flows (Figure 2). The stratigraphic section of the Newark basin (Figures 3a and b) ranges in age from middle Carnian (Triassic) to Hettangian-Sinemurian (Jurassic) and includes nine formations with a total thickness of more than 25,300 feet (7700 m). This section includes a thick sequence of predominantly clastic sedimentary rocks that contain three series of Lower Jurassic (Hettangian) basalt lava flows. The basalts of the Newark basin underlie a series of three ridges which constitute the Watchung Mountains in northern New Jersey. The ridges are flanked by lowlands formed on Lower Jurassic sedimentary rocks that underlie, overlie, and are intercalated with the three basalt series. Originally referred to as the First, Second,

and Third Watchung Basalts (from oldest to youngest) and included as part of the Brunswick Formation, these extrusive units have since been elevated to formation status and renamed the Orange Mountain, Preakness, and Hook Mountain Basalts in a stratigraphic revision proposed by Olsen (1980). These basalts occur exclusively within the uppermost one-fifth of the exposed stratigraphic section of the Newark basin (Figure 3b; Olsen and others, 1989). The Orange Mountain Basalt overlies approximately 20,350 feet (6200 m) of mostly Upper Triassic, predominantly clastic sedimentary rocks of the Stockton, Lockatong, and Passaic Formations and is separated from the Preakness Basalt by 558 feet (170 m) of sedimentary strata of the Feltville Formation (Figure 3b; see summary in Olsen and others, 1989, for additional information). The Preakness Basalt is separated from the Hook Mountain Basalt by 1115 feet (340 m) of sedimentary strata of the Towaco Formation, and the Hook Mountain Basalt is in turn overlain by at least 1640 feet (500 m) of clastic sedimentary rocks of the Boonton Formation.

Analytical Methods

One hundred and thirty-five samples were collected on the basis of position in the cores and relative degree of alteration. Representative samples were collected wherever physical evidence indicated a stratigraphic break (e.g. sedimentary intercalation, vesicular zone) or feature of unusual interest (e.g. gabbroids). In some instances, however, the relative degree of mineralogic alteration or presence of abundant secondary mineralization (amygdules, veins) prohibited use of selected samples for geochemical analysis. Of the one hundred and thirty-five samples collected, seventy-one samples were analyzed geochemically. Samples were split manually using a steel jaw splitter and approximately 100 grams were crushed by grinding in a shatterbox apparatus using a stainless steel vessel. Splits of these powders were analyzed for major elements and the trace elements Y, Sr, Rb, Pb, Ga, Nb, Zr, Zn, Ni, Cr, V, Ce, and Ba by X-ray fluorescence (XRF) at the University of Massachusetts at Amherst using modifications of the methods of Norrish and Chappell (1967) and Norrish and Hutton (1969). All samples were analyzed in duplicate. Estimates of the analytical precision (1 sigma) for the XRF data are based on analyses of selected duplicate pairs. The concentrations of all rare earth elements (REE) and the trace elements Th, Ta, and Hf were determined for forty-six samples through instrumental neutron

activation (INA) analysis performed at the analytical laboratories of the United States Geological Survey (USGS) in Reston, Virginia following procedures described by Baedecker and McKown (1987). Estimates of the analytical precision for these data are based on replicate analyses of the USGS rock standard BCR-1.

Description of Cores

Orange Mountain Basalt

Core PT-29 sampled the lower part of the Orange Mountain Basalt through a distance of 330 feet (100.6 m), penetrating the contact between the basalt and underlying redbeds of the Passaic Formation at a total depth of 349 feet (106.4 m) (Figure 4). The cored stratigraphic interval of 327.5 feet (99.8 m) represents approximately 66% of the total average thickness of 492 feet (150 m) of the Orange Mountain Basalt in the Newark basin (Olsen and others, 1989). Prominent amygdaloidal zones occurring at depth intervals 80-87 feet (24.4 - 26.5 m) and 116.5 - 149 feet (35.5 - 45.4 m) separate three distinct flow units (designated as OM-3, OM-2, OM-1, upper to lower, respectively; see Figure 4) comprising this sequence.

Preakness Basalt

The Preakness Basalt was sampled in cores PT-17, PT-18, PT-19, PT 20, and PTI-3 (Figures 5a-e). Core PT-17 penetrated the upper contact between the basalt and overlying redbeds of the Towaco Formation at a depth of 98 feet (29.6 m) and continued in basalt to a total depth of 222.5 feet (67.8 m). Prominent amygdaloidal zones at depth intervals 128-135 feet (39.0 - 41.1 m) and 174.5 - 212 feet (53.2 - 64.6 m) separate three flow units (designated as P-9, P-8, and P-7, upper to lower, respectively; see Table 1) in this portion of the Preakness Basalt. The deeply weathered and brecciated, amygdaloidal zone located at the top of the basalt suggests that nearly all of the uppermost flow has been preserved. Core PT-18 sampled a total stratigraphic interval of 135 feet (41.2 m). The prominent amygdaloidal zone located at the top of this core has been correlated with a similar zone occurring at depth interval 174.5 - 212 feet (53.2 - 64.6 m) in core PT-17 on the basis of structural, petrographic, and geochemical data, indicating a minimum stratigraphic thickness of 139 feet (42.4 m) for flow P-7 of the Preakness Basalt

(Table 1).

Core PT-19 sampled a total stratigraphic interval of 224 feet (68.2 m). Siltstone occurring within the depth interval 137-146 feet (41.8 - 44.5 m) separates two flows, designated as P-6 (upper) and P-5 (lower), respectively, in this core. Core PT-20 penetrated a stratigraphic interval of 271 feet (82.6 m) in basalt characterized by lack of textural evidence for interflow boundaries. The marked change in composition occurring in the interval 145-197 feet (44.2 - 60.0 m) is interpreted, however, to represent the boundary between two flows (designated as P-4 and P-3, upper and lower, respectively) erupted within a relatively short interval of time during which no appreciable weathering of the upper surface of the earlier flow took place. Four zones of discordant, coarse-grained gabbroid occur within the depth interval 60 - 125 feet (18.3 - 38.1 m). On the basis of other occurrences of similar gabbroids observed in basalts from the Culpeper (Tollo, 1988) and Hartford basins, these coarse-grained rocks are interpreted as late-stage auto-intrusions and/or possible segregations within the basalt.

Core PTI-3 sampled a stratigraphic section measuring 114 feet (34.8 m) in the lower portion of the Preakness Basalt, penetrating the contact with sandstone of the underlying Feltville Formation at a depth of 119 feet (36.3 m). An amygdaloidal/vesicular zone located in the depth interval 73-80 feet (22.3 - 24.4 m) in this core separates the lowermost two flows (designated P-2 and P-1, upper and lower, respectively) of the Preakness sequence. A total minimum stratigraphic thickness (including intercalated sedimentary strata) of 815.2 feet (248.5 m) was sampled by these five cores. This represents approximately 99% of the average total thickness of the Preakness Basalt, which has been estimated to be 820 feet (250 m) thick (Olsen and others, 1989). Structural and petrochemical data suggest that minor stratigraphic gaps may be present between cores PT-18, PT-19, PT-20, and PTI-3.

Hook Mountain Basalt

The Hook Mountain Basalt was sampled in cores PT-10 and PT-11 (Figures 6a and 6b). Core PT-10 penetrated the contact between the basalt and redbeds of the overlying Boonton Formation at a depth of 136 feet (41.4 m) and continued in basalt to a total depth of 211 feet (64.0 m), representing a stratigraphic interval in basalt of approximately 74.4 feet

(22.7 m). Core PT-11 traversed the lower portion of the basalt over a distance of 243 feet (74.0 m), representing a stratigraphic interval of 241.2 feet (73.5 m), and penetrated redbeds of the underlying Towaco Formation at a depth of 255 feet (77.6 m). A prominent weathered flow top and an amygdaloidal zone at depth interval 162-193 feet (49-59 m) separate two flow units (designated as HM-2 and HM-1, upper and lower, respectively; see Table 1) in core PT-11. The basalt in core PT-10 contains several minor vesicular zones which may separate individual surges within the uppermost flow unit.

Structural and geochemical data (Tollo and Gottfried, in press) suggest that the upper flow unit in core PT-11 correlates with the basalt in core PT-10. The stratigraphic interval of 315.6 feet (96.2 m) of basalt sampled in these two cores is slightly less than the thickness estimated for the Hook Mountain Basalt by Olsen and others (1989), suggesting that a small gap (probably in flow HM-2) occurs between the cored sections.

Medium- to coarse-grained, locally vesicular and amygdaloidal, porphyritic plagioclase + clinopyroxene diabase and gabbroid occurs in both the PT-10 and PT-11 cores (Figures 6a and 6b). The gabbroids appear to be generally concordant with the regional structure and are interpreted to represent late-stage auto-intrusions or possible segregations within the basalt.

Petrography

The three basalt formations of the Newark basin are petrographically distinct, as shown by the data summarized in Tables 2 and 3. The Orange Mountain Basalt is finer grained than either the Preakness or Hook Mountain Basalts and is characterized by glomeroporphyritic texture defined by rounded clusters of subhedral to euhedral augite locally intergrown with subhedral plagioclase. Iron -titanium oxide phases in the Orange Mountain Basalt typically occur as trellis-shaped or skeletal grains restricted to the mesostasis. The mesostasis is brown and locally comprises as much 10% of the total volume of individual samples.

The flow units of the Preakness Basalt display a range of petrographic characteristics (Table 3). Porphyritic textures are common

with plagioclase and clinopyroxene as the dominant phenocryst phases. In general, the Preakness exhibits the coarsest average grain size of the three series (excluding the gabbroids) and includes the highest modal percentage of micropegmatite. Iron-titanium oxide phases range from blocky and possibly phenocrystic to finely granular. The mesostasis is typically light brown and comprises as much as 5% of the mode. The Preakness is the only basalt (gabbroids excluded) to contain augite displaying herringbone twinning. The coarse-grained gabbroids that occur within the Preakness Basalt in core PT-20 contain the assemblage plagioclase + augite + pigeonite + iron-titanium oxide. The pyroxenes are typically distinctive in the gabbroids, forming elongate, locally curved blades as much as 2 inches (5 cm) in length. Contacts between the gabbroids and adjacent basalt vary from locally sharp to gradational.

The Hook Mountain Basalt is typically intermediate in grain size between the Orange Mountain and Preakness Basalts and locally exhibits aphyric, microporphyritic, and glomeroporphyritic texture. Iron-titanium oxide phases occur as (presumably early crystallizing) blocky grains, as (late crystallizing) skeletal to dendritic grains restricted to the mesostasis, or as both. Coarse-grained gabbroids, which are texturally similar to those described above, occur at several locations within the PT-11 core. These distinctive rocks typically exhibit both sharp and gradational contacts and are petrographically similar to the enclosing Hook Mountain Basalt except for the characteristic coarse grain size and locally vesicular nature of the gabbroids.

The Preakness and Hook Mountain Basalts include petrographically distinct subtypes which generally correspond to the individual flow units defined by differences in physical properties and chemical composition. Distinctive petrographic characteristics include 1) overall grain size, 2) gross texture, 3) groundmass texture, 4) modal percentage and relative proportion of phenocrysts, 5) relative proportion of groundmass constituents, and 6) the habit of the iron-titanium oxide phases. These characteristics support the correlation of flow HM-2 between cores PT-10 and PT-11, and flow P-7 between cores PT-17 and PT-18.

Geochemistry

Geochemical data for the individual samples analyzed in this study are presented in Table 4. Most of the data represent averages of replicate analyses performed on separate sample splits (see analyses in Table 4). These data form the entire database used for the discussion in Tollo and Gottfried (in press). Data for samples PT29-348 annd PT11-254 were excluded by these authors from the statistical calculations of the Orange Mountain and Hook Mountain Basalts, respectively, due to obvious chemical effects related to the proximity of each sample to the contact with underlying sedimentary strata.

References Cited

Anders, E., and Ebihara, M., 1982, Solar system abundances of the elements: Geochemica et Cosmochimica Acta; v. 46, p. 2363-2380.

Baedecker, P.A., and McKown, D.M., 1987, Instrumental neutron activation analysis of geochemical samples, *in* P.A. Baedecker (ed.), Methods for Geochemical Analysis. U.S. Geological Survey Bulletin 1770, p. H1-H14.

Fedosh, M.S., and Smoot, J.P., 1988, A cored stratigraphic section through the northern Newark basin, *in* A.J. Froelich, and G.R. Robinson, Jr. (eds.), Studies of the early Mesozoic basins of the Eastern United States, U.S. Geological Survey Bulletin 1776, p. 19-24.

Norrish, K., and Chappell, B.W., 1967, X-ray fluorescence spectrography *in* Zussman, J. (ed.), Physical Methods in Determinative Mineralogy, Academic Press, Orlando, p. 161-214.

Norrish, K., and Hutton, J.T., 1969, An accurate X-ray spectrographic method for the analysis of a wide range of geological samples: Geochemica et Cosmochimica Acta, v. 33, p. 431-454.

Olsen, P.E., 1980, The Latest Triassic and Early Jurassic formations of the Newark basin (Eastern North America, Newark Supergroup): Stratigraphy, Structure, and Correlation: Bulletin, New Jersey Academy of Science, v. 25, no. 2, p. 25-51.

Olsen, P.E., Schlishe, R.W., and Gore, P.J.W., (eds.), 1989, Tectonic, depositional, and paleoecological history of early Mesozoic rift basins, Eastern North America: Field Trip Guidebook T351, 28th International Geological Congress, American Geophysical Union, Washington, DC, 174 p.

Tollo, R.P., 1988, Petrographic and major-element characteristics of Mesozoic basalts, Culpeper basin, Virginia, *in* A.J. Froelich, and G.R. Robinson, Jr. (eds.), Studies of the early Mesozoic basins of the Eastern United States, U.S. Geological Survey Bulletin 1776, p. 105-113.

Tollo, R.P., and Gottfried, D., in press, Petrochemistry of Jurassic basalt from eight cores, Newark basin, New Jersey: Implications for the petrogenesis of Newark Supergroup volcanics, Geological Society of America.

Figure Captions

Figure 1: Generalized geologic map of part of the Newark basin, New Jersey, showing locations of core hole sites.

Figure 2: Map showing the distribution of exposed early Mesozoic basins in the eastern United States and major occurrences of early Jurassic basalt.

Figure 3a and b: Schematic stratigraphic column for the Newark basin (3a) showing intervals of the Lower Jurassic section penetrated by the cores examimed in this study (3b). Thickness data are from Olsen and others (1989).

Figure 4: Schematic columnar section of the interval penetrated by core PT-29 in the Orange Mountain Basalt, showing major lithologic features and positions of samples collected. All numbers refer to distance (in feet) from the top of the core.

Figures 5a-e: Schematic columnar sections of the intervals penetrated by cores PT-17 (5a), PT-18 (5b), PT-19 (5c), PT-20 (5d), and PTI-3 (5e) in the Preakness Basalt, showing major lithologic features and positions of samples collected. All numbers refer to distance (in feet) from the top of the core.

Figures 6a-b: Schematic columnar sections of the interval penetrated by cores PT-10 (7a) and PT-11 (7b) in the Hook Mountain Basalt, showing major lithologic features and positions of samples collected. All numbers refer to distance (in feet) from the top of the core.

Figure 1

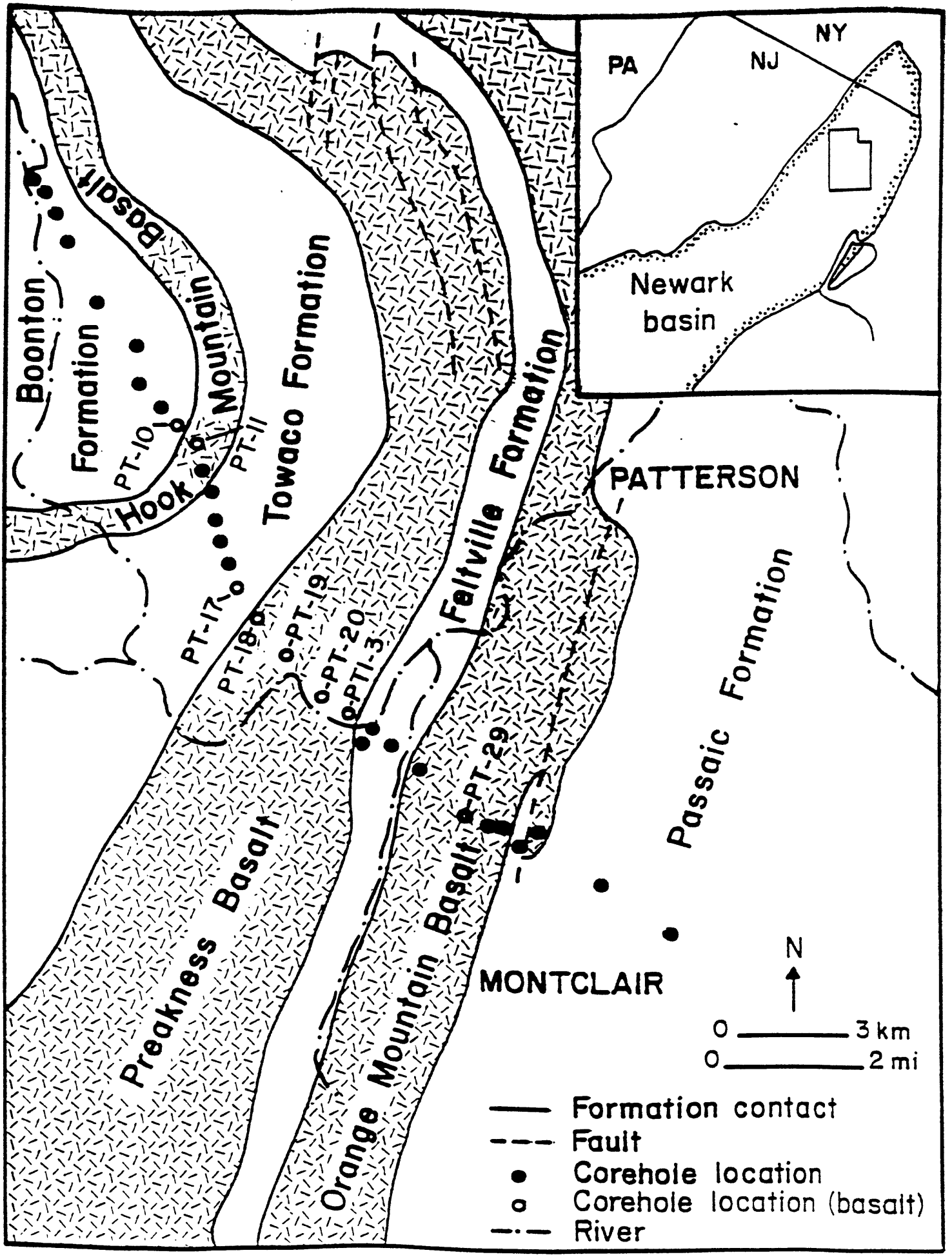
NY
PA
NJ
Newark basin
Boonton Formation
Boonton
Hook Mountain
Towaco Formation
Feltville Formation
PATTERSON
Passaic Formation
MONTCLAIR
Preakness Basalt
Orange Mountain Basalt
PT-10
PT-11
PT-17
PT-18
PT-19
PT-20
PTI-3
PT-29
N
0 3 km
0 2 mi
Formation contact
Fault
Corehole location
Corehole location (basalt)
River

Figure 2

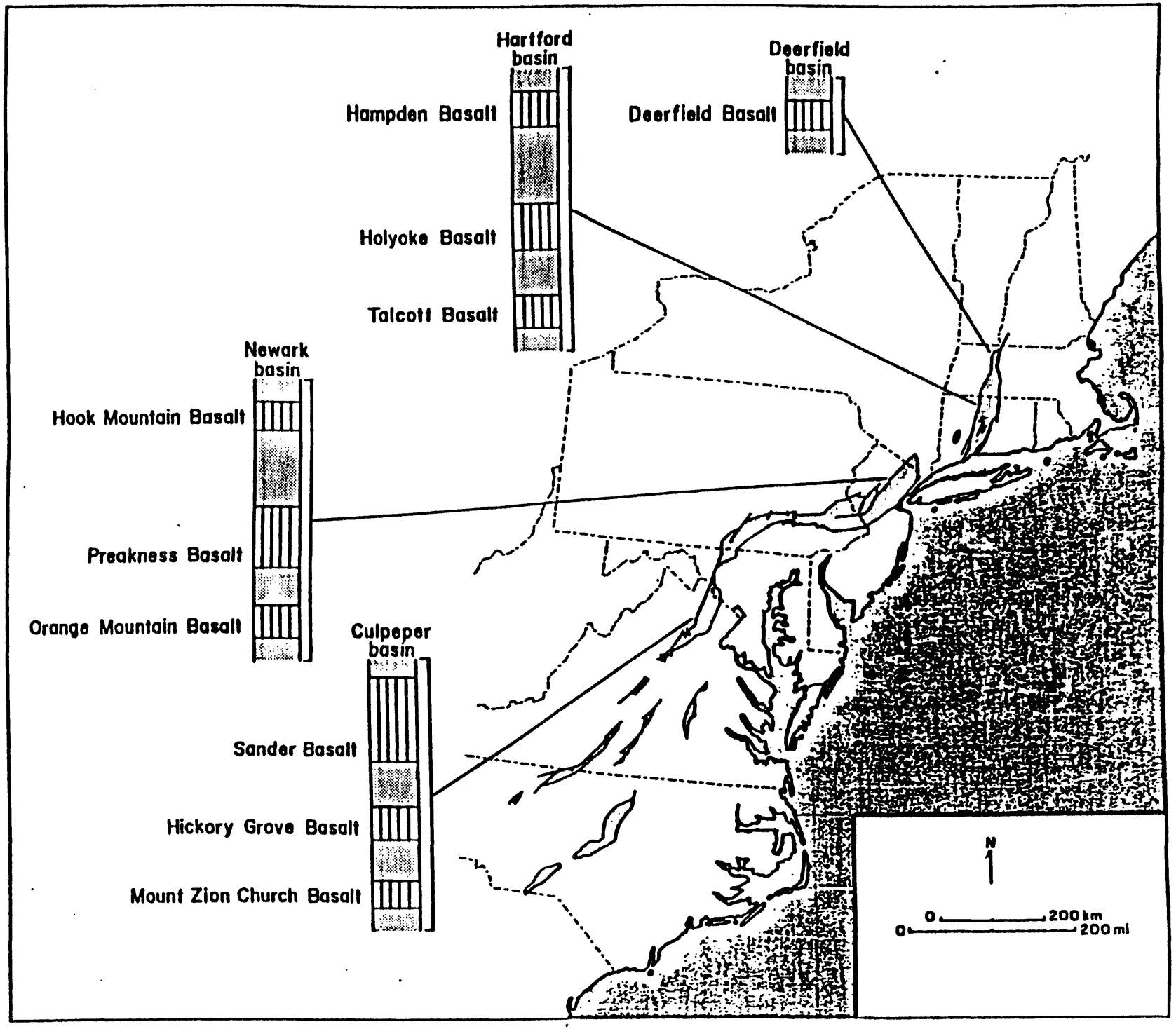
Hartford basin
Hampden Basalt
Holyoke Basalt
Talcott Basalt
Deerfield basin
Deerfield Basalt
Newark basin
Hook Mountain Basalt
Preakness Basalt
Orange Mountain Basalt
Culpeper basin
Sander Basalt
Hickory Grove Basalt
Mount Zion Church Basalt
N
0 200 km
0 200 mi

Figure 3b

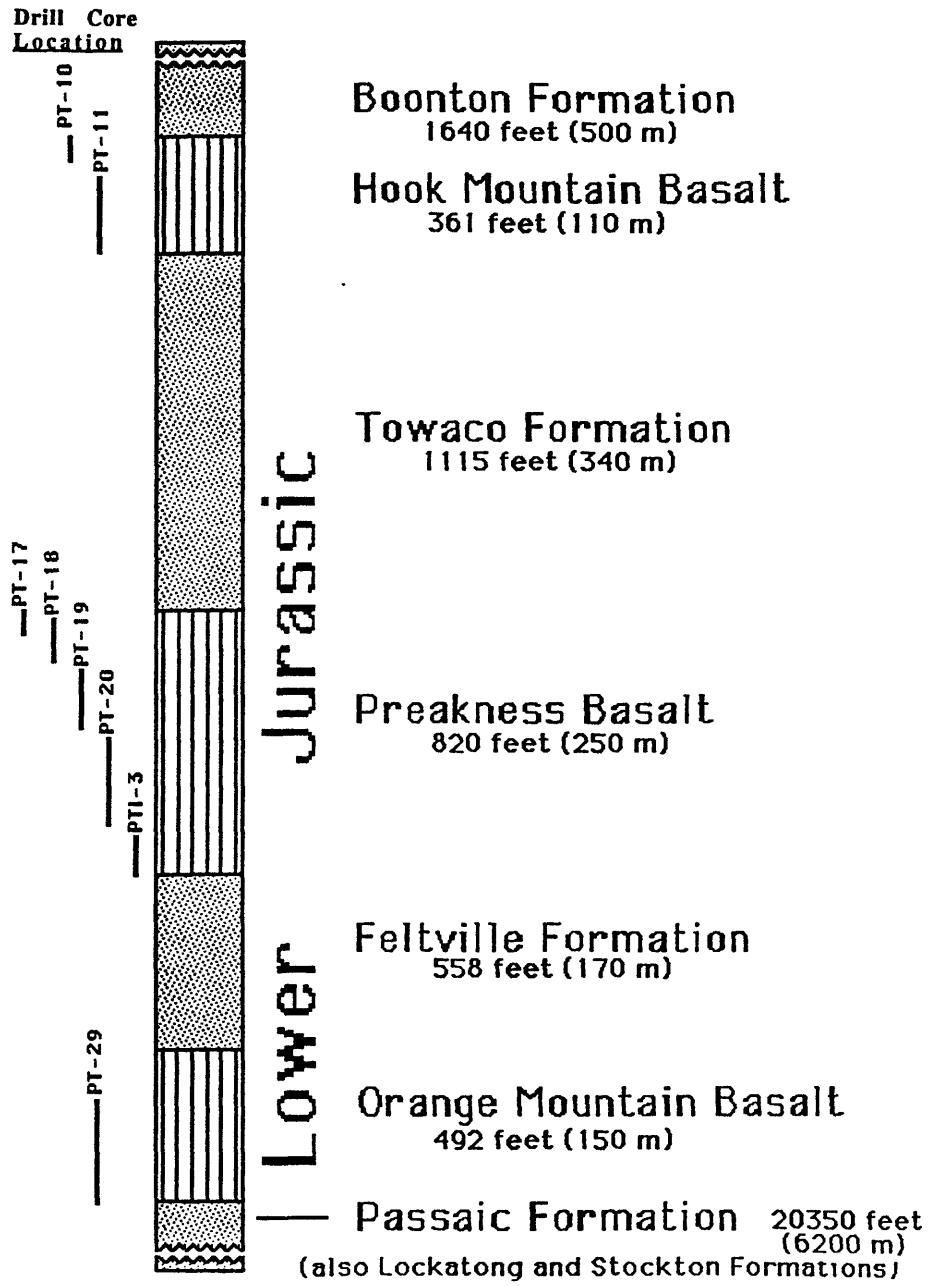

Figure 3a

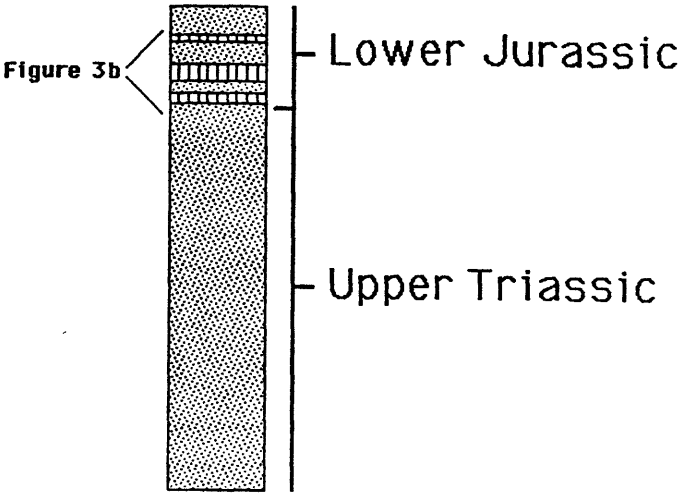

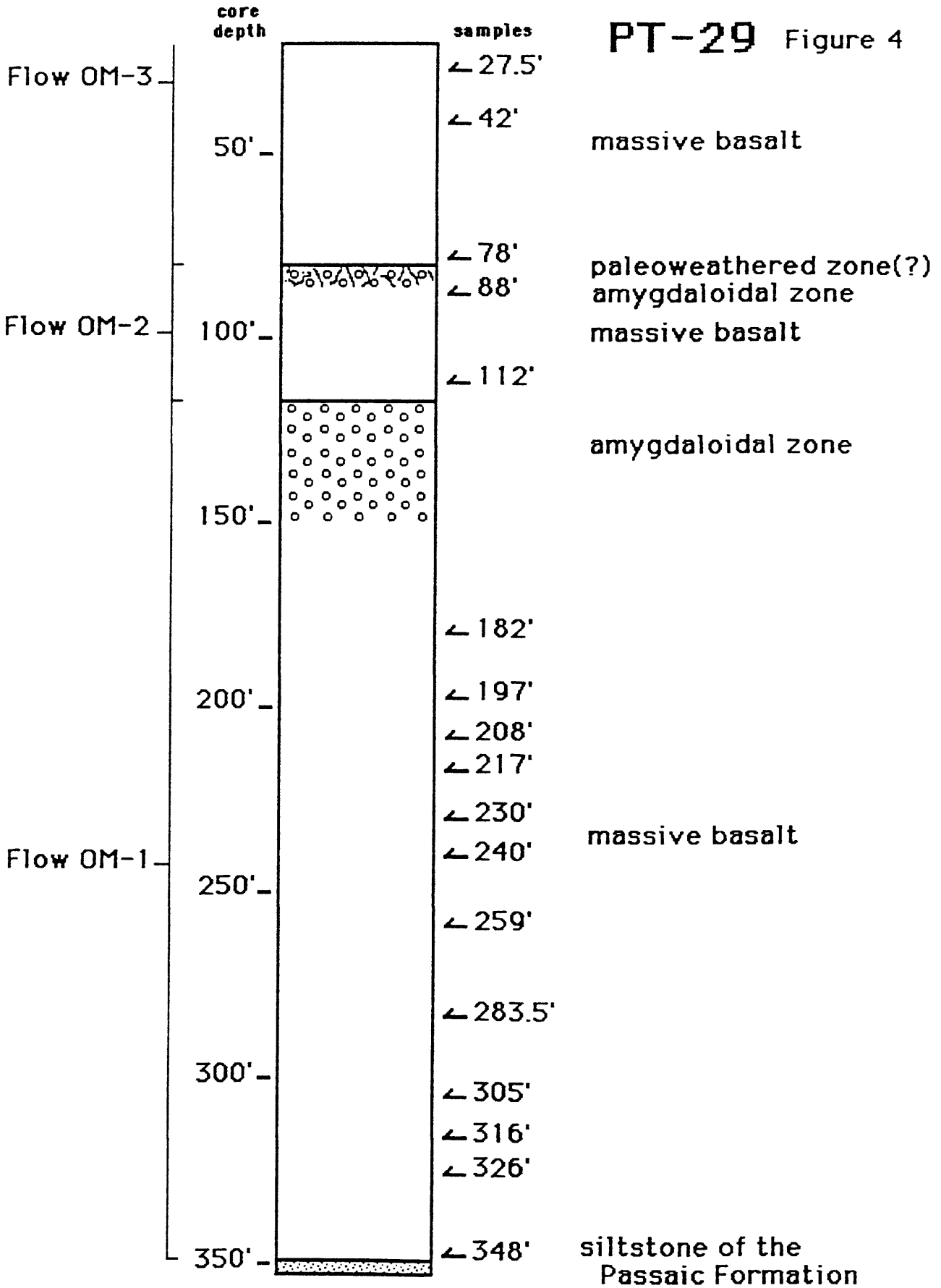
core depth
samples
PT-29 Figure 4
Flow OM-3
Flow OM-2
Flow OM-1
50'
100'
150'
200'
250'
300'
350'
27.5'
42'
78'
88'
112'
182'
197'
208'
217'
230'
240'
259'
283.5'
305'
316'
326'
348'
massive basalt
paleoweathered zone(?)
amygdaloidal zone
massive basalt
amygdaloidal zone
massive basalt
siltstone of the Passaic Formation

PT-17 Figure 5a

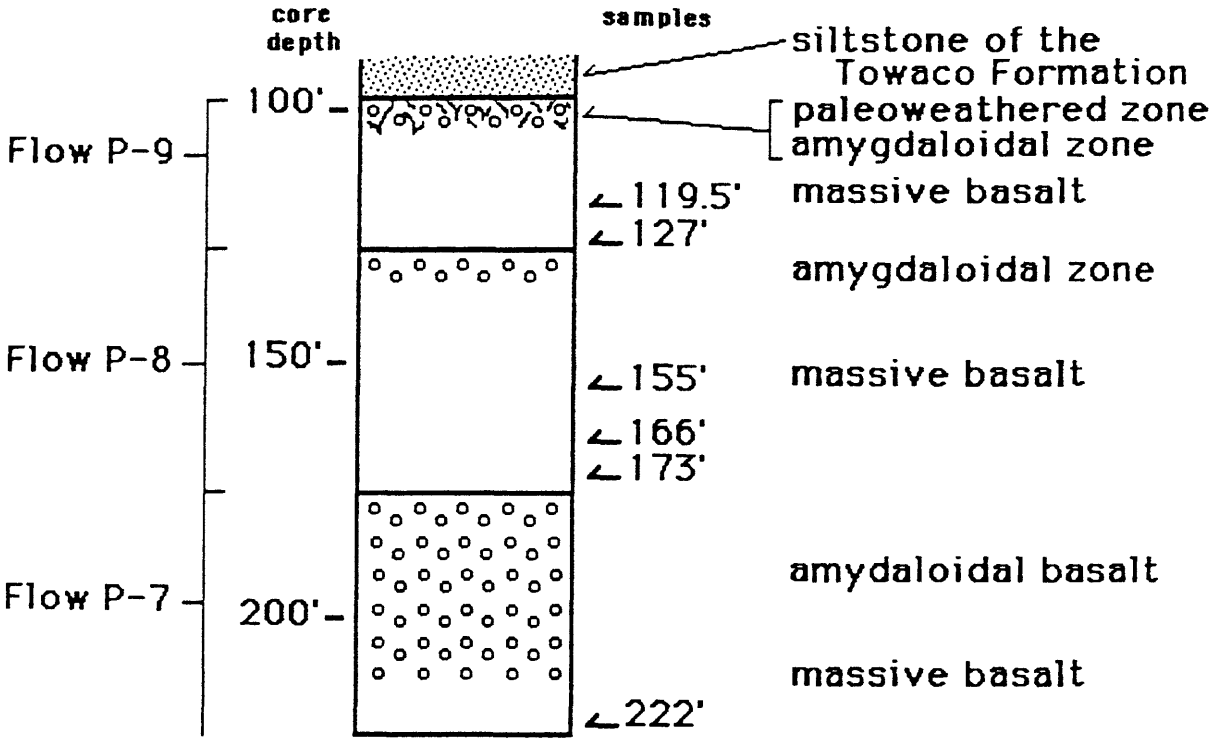

PT-18 Figure 5b

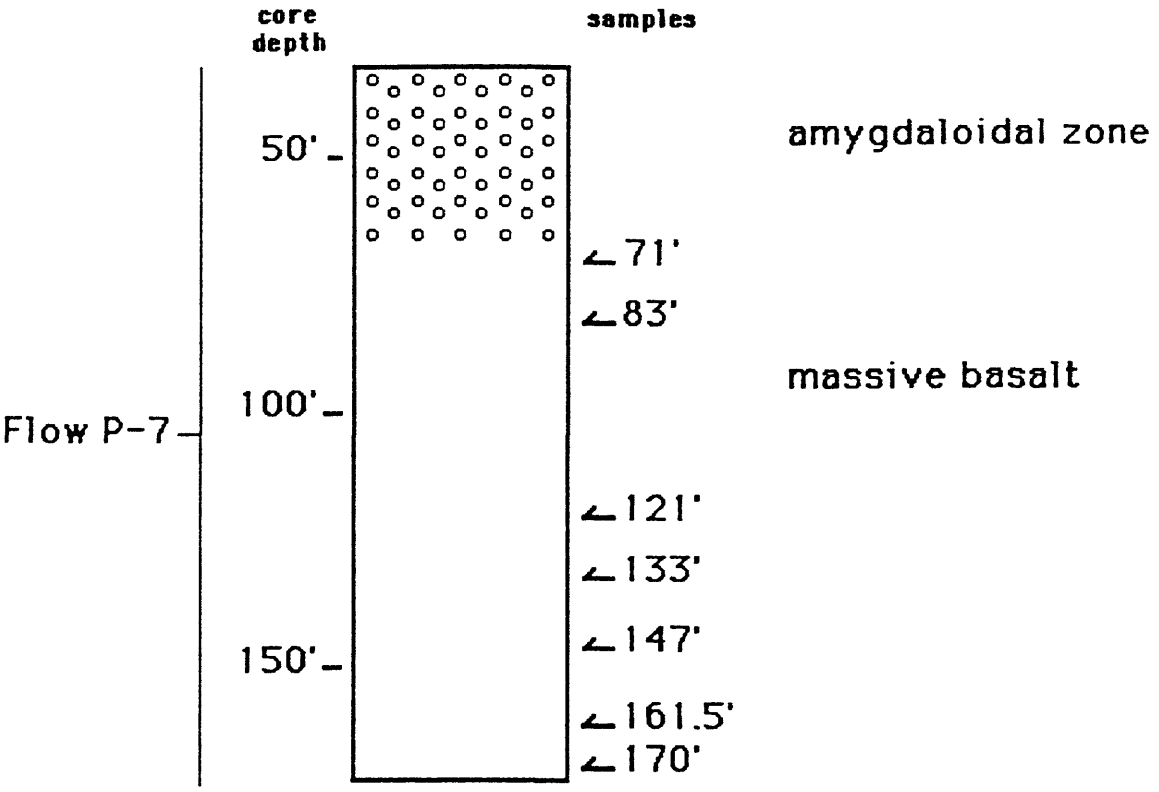

PT-19 Figure 5c

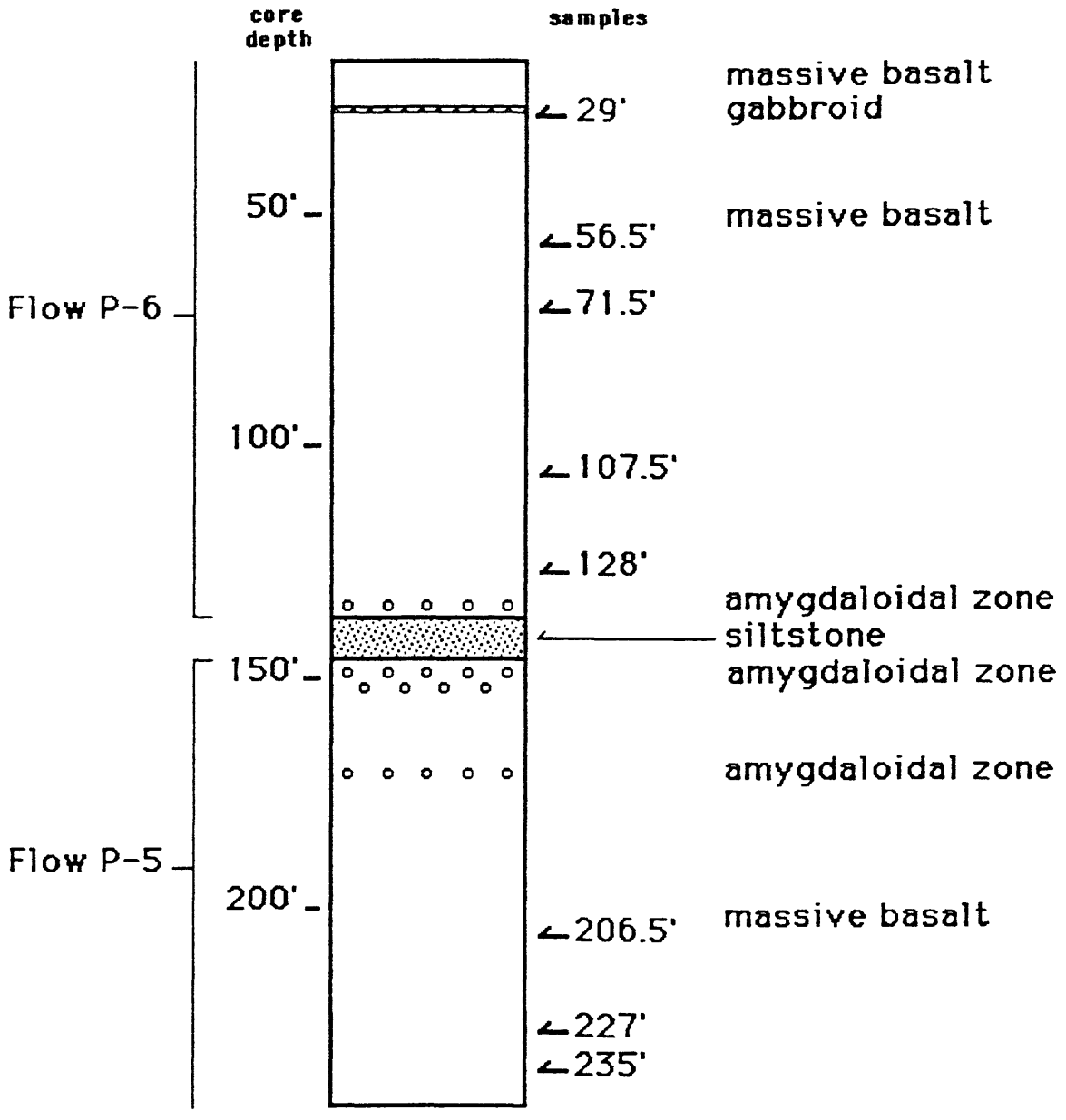

PT-20 Figure 5d

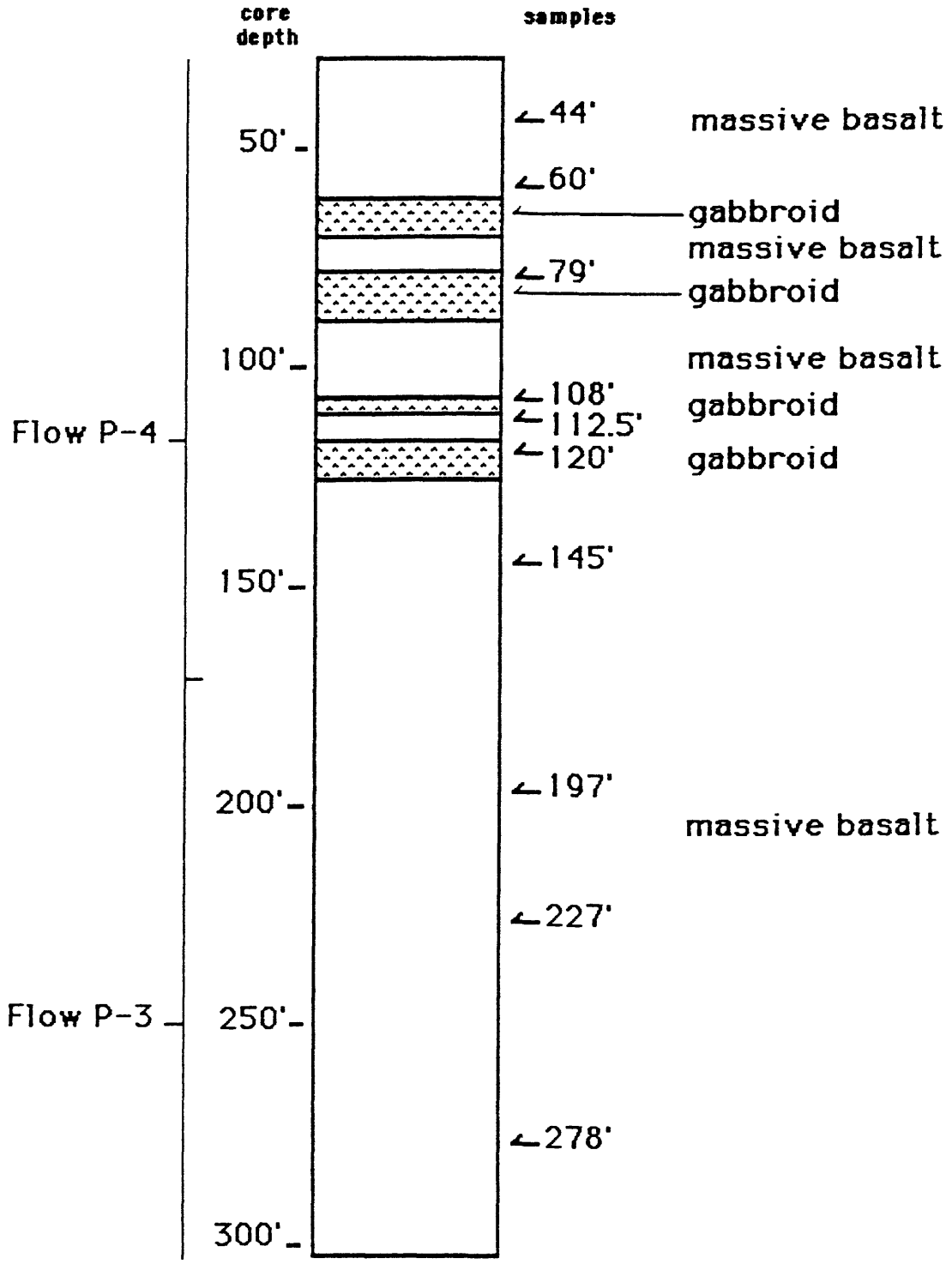

PTI-3 Figure 5e

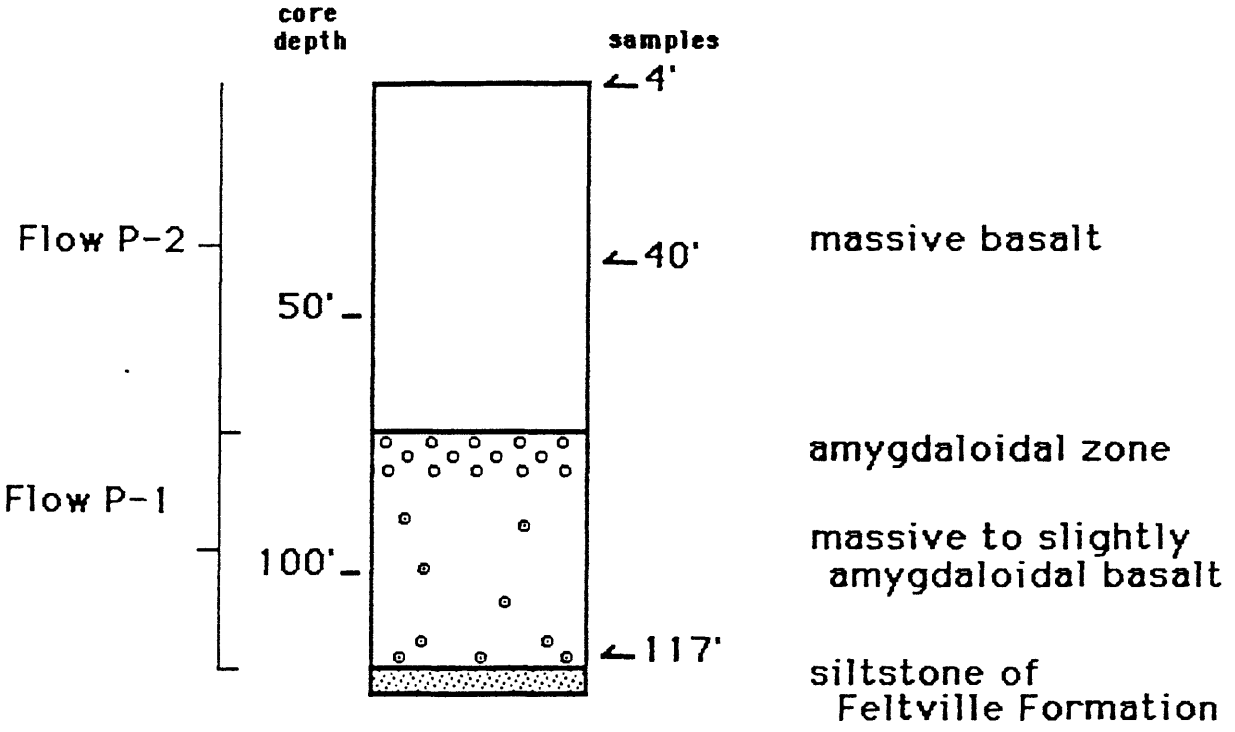

PT-10 Figure 6a

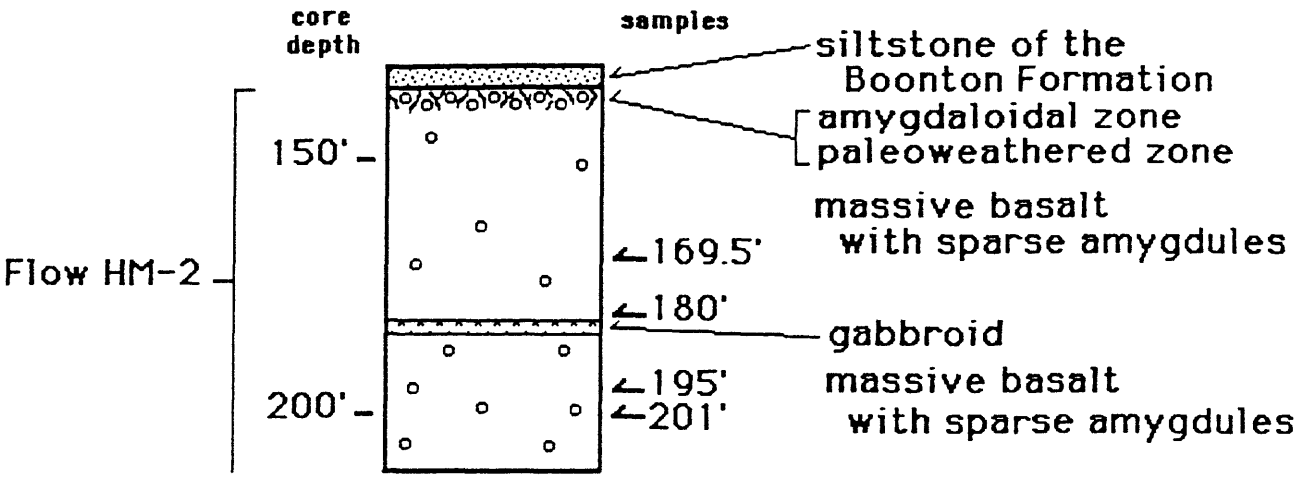

PT-11 Figure 6b

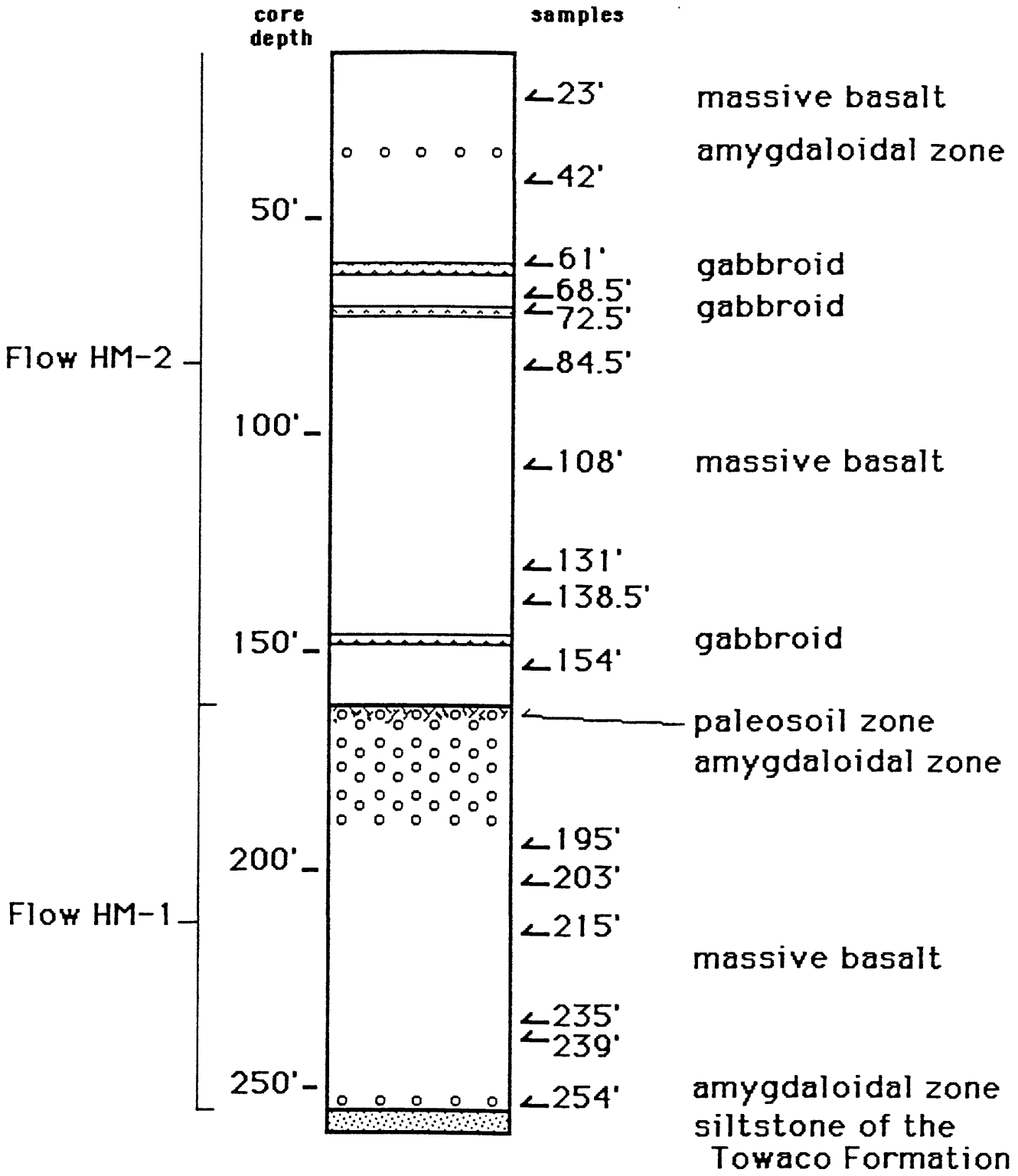

Table 1: Summary of thickness data for individual flow units within the Newark basin cores.

Formation	Flow #	Core	Interval in core	Stratigraphic thickness*	Remarks
Hook Mountain Basalt	HM-2	PT-10	136-211 ft	>74.4 ft (22.7 m)	probable gap in section between the two cores
		PT-11	12-162.5 ft	>149.4 ft (45.5 m)	
	HM-1	PT-11	162.5-255 ft	91.8 ft (28.0 m)	entire flow sampled
Preakness Basalt	P-9	PT-17	98-128 ft	29.8 ft (9.1 m)	entire flow sampled
	P-8	PT-17	128-174.5 ft	46.2 ft (14.1 m)	entire flow sampled
	P-7	PT-17	174.5-222.5 ft	overlap	amygdaloidal flow top correlated between cores
		PT-18	32-172 ft	>139.0 ft (42.4 m)	
	P-6	PT-19	16.5-137 ft	>119.6 ft (36.5 m)	uppermost portion not sampled
	P-5	PT-19	146-242 ft	>95.3 ft (29.0 m)	lowermost portion not sampled
	P-4	PT-20	29-171 ft	<>140.1 ft (42.7 m)	uppermost portion not sampled lower contact inferred on basis of compositional change contains abundant coarse-grained gabbroids
	P-3	PT-20	171-303 ft	<>131.0 ft (39.9 m)	lowermost portion not sampled upper contact inferred on basis of compositional change
	P-2	PTI-3	4-73 ft	>68.5 ft (20.9 m)	uppermost portion not sampled
	P-1	PTI-3	73-119 ft	45.7 ft (13.9 m)	entire flow sampled
Orange Mountain Basalt	OM-3	PT-29	19-80 ft	>60.5 ft (18.5 m)	uppermost portion not sampled
	OM-2	PT-29	80-116.5 ft	36.2 ft (11.1 m)	entire flow sampled
	OM-1	PT-29	116.5-349 ft	230.8 ft (70.3 m)	lowermost portion not sampled

* calculated assuming dip of 7° throughout the section

Table 2: General petrographic characteristics of the three basalt series of the Newark basin cores.

	Orange Mountain Basalt	Preakness Basalt	Hook Mountain Basalt
grain size	aphanitic to fine-grained	fine- to coarse-grained	fine- to medium-grained
texture	microporphyritic glomeroporphyritic	aphyric microporphyritic glomeroporphyritic	aphyric seriate glomeroporphyritic
phenocryst characteristics	≤10 % of mode aug + plag 10 : 1 ratio euhedral to subhedral <2.5 mm	≤5% of mode plag ± aug ± Fe-Ti oxide 2 : 1 : 1 ratio euhedral to subhedral <2.5 mm	≤10 % of mode plag + aug ± pig 3 : 1 : tr ratio euhedral to subhedral <2.5 mm
groundmass characteristics	intersertal plag + aug + Fe-Ti oxide 1 : 1 : 0.5 ratio plag + aug: ≤0.5 mm Fe-Ti oxide: ≤0.1 mm	intergranular to subophitic plag + aug + pig + Fe-Ti oxide 2 : 2 : 0.5 : tr ratio plag + aug + Fe-Ti oxide: ≤1 mm pig: ≤0.6 mm	intergranular to subophitic plag + aug + pig + Fe-Ti oxide 1 : 1 : 0.5 : 0.5 ratio ≤1.5 mm
Fe-Ti Oxide characteristics	restricted to mesostasis very fine-grained trellis-shaped, skeletal, dusty	fine-grained and blocky or restricted to mesostasis and dendritic, skeletal, or dusty	fine-grained and blocky, very fine-grained and granular or restricted to mesostasis and skeletal or dendritic
groundmass characteristics	≤10% of mode brown, turbid, with local perlitic fractures	≤5% of mode light brown, turbid contains apatite ± Fe-Ti oxides	≤5% of mode light brown to colorless contains apatite ± Fe-Ti oxides
secondary minerals	chl, serp, serc, saus, cal, zeol	chl, serp, serc, saus, lim, cal, zeol	chl, serp, serc, saus, lim, cal, zeol
remarks	1) glomeroporhyritic clusters may be rounded, locally contain plag; 2) plag phenocrysts are zoned with calcic cores; 3) plag comp: An57-An62; 4) serpentinized olivine relics occur as phenocrysts and in groundmass.	1) aug exhibits herringbone twinning: 2) micropegmatite comprises ≤2% of mode; 3) zoned plag with calcic cores; 4) plag comp: An50-An55.	1) aug does not exhibit herringbone twinng; 2) zoned plag with calcic cores; 3) plag comp: An62-An65.

abbreviations include tr:trace; plag:plagioclase; aug:augite, pig:pigeonite; chl:chlorite; serp:serpentine; serc:sericite; saus:saussurite; cal:calcite; lim:limonite; zeol:zeolites.

Table 3: Detailed petrographic characteristics of individual flow units in the three basalt series of the Newark basin cores.

Series	Flow Unit	Core	Grain Size	Texture	Phenocrysts	Groundmass	Fe-Ti Oxides
Hook Mountain Basalt	HM-2	PT10, PT11	fine to medium	glomeroporphyritic, intergranular, seriate, subophitic, aphyric	2% plag + aug 3 : 1 to 2 : 1 ratio <2.5 mm	plag + aug + pig 1 : 1 : 0.5 ratio	blocky <1 mm
	HM-1	PT11	fine	glomeroporphyritic, intergranular, subophitic	8% plag + aug 5 : 1 ratio <1.5 mm	plag + aug + pig 1 : 1 : 0.5 ratio	interstitial, finely granular, skeletal locally granular
Preakness Basalt	P-9 P-8 P-7	PT17 PT17 PT-17, PT18	very fine to fine	aphyric to sparcely porphyritic	(trace) plag	plag + aug + pig 2 : 2 : 0.5 ratio	interstitial, finely granular
	P-6	PT19	fine to medium	porphyritic intergranular	3% aug + Fe-Ti oxide ± plag 2 : 0.5 : trace <2.5 mm	plag + aug + pig 2 : 1: 0.5 ratio	blocky phenocrysts and groundmass
	P-5	PT19	medium	glomeroporphyritic, intergranular, subophitic	3% plag ± aug <2.5 mm	plag + aug + pig 2 : 1: 0.5 ratio	mesostasis only, granular and skeletal
	P-4 P-3	PT20 PT20	medium to coarse	aphyric, intergranular, subophitic	none	plag + aug + pig + Fe-Ti oxide 1 : 1 : 0.5 : trace	blocky
	P-2 P-1	PTI-3 PTI-3	fine to medium	glomeroporphyritic, intergranular, subophitic	3% plag ± aug <2.5 mm	plag + aug + pig 2 : 1: 0.5 ratio	blocky, locally interstitial and skeletal
Orange Mountain Basalt	OM-3 OM-2 OM-1	PT-29 PT-29 PT-29	aphanitic to fine	glomeroporphyritic, to porphyritic	<10% aug + plag 10 : 1 ratio <2.5 mm	plag + aug + Fe-Ti oxide 1 : 1 : 0.5	mesostasis only, finely granular to skeletal

Table 4: Geochemical data for individual samples. Major elements expressed in weight percent; trace elements in parts per million.

Orange Mountain Basalt

Sample:	PT-29-27.5	PT-29-42	PT-29-78	PT-29-88	PT-29-112	PT-29-182	PT-29-197	PT-29-208	PT-29-217	PT-29-230	PT-29-240	PT-29-259	PT-29-283.5
SiO2	51.99	51.77	52.66	52.97	52.44	52.07	52.72	52.11	52.00	52.41	52.23	52.41	52.06
TiO2	1.15	1.16	1.14	1.15	1.12	1.10	1.11	1.12	1.12	1.11	1.10	1.10	1.09
Al2O3	14.33	14.23	14.08	14.53	14.30	13.97	14.18	14.28	14.32	14.19	14.11	14.17	13.95
Fe2O3*	11.61	11.33	10.99	11.35	11.12	11.57	10.96	11.19	11.23	11.19	11.13	11.26	11.26
MnO	0.16	0.18	0.18	0.16	0.17	0.19	0.18	0.17	0.17	0.18	0.17	0.18	0.18
MgO	7.79	7.81	7.14	7.96	7.30	7.71	7.40	7.72	7.74	7.77	7.74	7.84	7.80
CaO	9.27	8.82	9.10	6.19	8.77	8.34	11.27	11.51	11.45	11.23	11.17	11.26	11.23
Na2O	3.62	4.24	3.91	5.34	4.27	4.37	2.02	1.97	1.96	2.06	2.08	2.13	2.26
K2O	0.51	0.54	0.64	0.20	0.70	0.52	0.24	0.30	0.38	0.31	0.30	0.27	0.27
P2O5	0.13	0.13	0.13	0.13	0.13	0.13	0.13	0.13	0.13	0.13	0.12	0.13	0.13
Total	100.56	100.21	99.97	99.98	100.32	99.97	100.21	100.50	100.50	100.58	100.15	100.75	100.23
analyses:	2	2	2	2	1	2	2	2	2	2	2	2	2
MI	59.8	59.2	60.6	58.8	60.4	60.0	59.7	59.2	59.2	59.0	59.0	59.0	59.1
Rb	16	19	20	7	25	22	6	8	11	12	13	13	14
Ba									125	117	124	128	118
Sr	163	217	152	235	162	271	181	179	179	191	192	185	184
Pb	6	6	5	5	5	6	5	7	10	6	6	6	6
Th	2		2		2		2		2	2		2	
Zr	104	102	102	101	100	99	100	100	101	100	99	98	99
Hf	2.6		2.5		2.3		2.4		2.4	2.4		2.3	
Nb	7.0	7.0	7.7	7.2	6.9	7.0	7.2	7.2	7.0	6.6	6.8	7.6	6.4
Ta	0.45		0.51		0.52		0.51		0.46	0.55		0.51	
Ni	104	99	105	102	100	95	104	102	99	104	108	108	94
Zn	84	88	98	92	92	90	85	84	84	84	81	83	83
Cr	303	297	333	304	306	283	304	313	310	345	338	174	353
Ga	17	18	17	14	16	14	17	17	17	17	18	17	17
V	254	248	250	247	253	247	252	253	253	244	241	241	243
La	9.7		9.5		8.8		9.9		10.2	10.2		10.2	
Ce	21.4		22.0		21.0		22.0		22.1	22.1		21.7	
Nd	11.9		12.2		11.5		11.8		12.5	12.2		11.3	
Sm	3.3		3.4		3.3		3.3		3.4	3.4		3.4	
Eu	1.0		1.0		1.0		1.0		1.1	1.0		1.0	
Tb	0.67		0.61		0.61		0.65		0.67	0.60		0.59	
Yb	2.0		2.1		2.0		2.1		2.1	2.1		2.1	
Lu	0.29		0.29		0.28		0.30		0.30	0.31		0.31	
Y	21.5	20.7	21.1	21.2	20.4	19.9	20.5	20.4	20.1	20.6	20.4	20.3	20.7
La(n)	31.4		30.7		28.4		32.8		33.0	33.1		32.9	
Yb(n)	9.7		10.2		9.7		10.1		10.0	10.1		10.3	
100Nb/Ti	0.10	0.10	0.11	0.10	0.10	0.11	0.11	0.11	0.10	0.10	0.10	0.12	0.10
Hf/Ta	5.73		4.80		4.44		4.61		5.30	4.33		4.51	
Th/Hf	0.79		0.90		0.86		0.87		0.83	0.86		0.86	
La(n)/Yb(n)	3.24		3.02		2.92		3.25		3.29	3.29		3.20	

Remarks

MI = 100*(Fe2O3*/(Fe2O3* + MgO))

* total iron expressed as Fe2O3; n.a. : not analyzed

(n) : normalized to chondritic abundances (Anders and Ebihara, 1982)

Table 4: (continued)

Orange Mountain Basalt

Sample:	PT-29-305	PT-29-316	PT-29-326	PT-29-348	Average	Std Dev	Maximum	Minimum
SiO2	51.78	52.28	52.86	49.50	52.13	0.77	52.97	49.50
TiO2	1.09	1.10	1.17	1.33	1.13	0.06	1.33	1.09
Al2O3	14.01	14.11	14.20	15.85	14.28	0.43	15.85	13.95
Fe2O3*	11.16	11.17	10.92	8.85	11.08	0.60	11.61	8.85
MnO	0.19	0.19	0.17	0.23	0.18	0.02	0.23	0.16
MgO	7.75	7.75	8.04	5.61	7.58	0.56	8.04	5.61
CaO	11.17	11.21	8.04	16.24	10.37	2.19	16.24	6.19
Na2O	2.07	2.20	3.57	2.32	2.96	1.12	5.34	1.96
K2O	0.25	0.24	1.69	0.34	0.45	0.35	1.69	0.20
P2O5	0.13	0.13	0.12	0.14	0.13	0.00	0.14	0.12
Total	99.60	100.38	100.78	100.41	100.30			
analyses:	2	2	2	2	samples	17		
MI	59.0	59.0	57.6	61.2	59.3	0.7	60.6	57.6
Rb	13	11	42	7	15	9	42	6
Ba	117	105		216	131	35	216	105
Sr	192	197	158	182	189	29	271	152
Pb	7	6	6	4	6	1	10	4
Th	2		2	2	2	0	2	2
Zr	97	99	95	98	100	2	104	95
Hf	2.5		2.3	2.5	2.4	0.1	2.6	2.3
Nb	6.5	7.2	6.5	7.6	7.0	0.4	7.7	6.4
Ta	0.53		0.54	0.56	0.51	0.04	0.56	0.45
Ni	94	94	90	85	99	6	108	85
Zn	82	83	79	224	94	34	224	79
Cr	341	320	324	350	311	41	353	174
Ga	17	18	15	17	16	1	18	14
V	239	240	235	262	247	7	262	235
La	10.3		10.0	10.7	9.9	0.5	10.7	8.8
Ce	22.2		21.5	22.9	21.9	0.5	22.9	21.0
Nd	12.1		11.0	11.9	11.8	0.5	12.5	11.0
Sm	3.4		3.3	3.5	3.4	0.1	3.5	3.3
Eu	1.1		1.0	1.1	1.0	0.0	1.1	1.0
Tb	0.59		0.61	0.58	0.62	0.03	0.67	0.58
Yb	2.1		2.1	2.2	2.1	0.0	2.2	2.0
Lu	0.30		0.30	0.32	0.30	0.01	0.32	0.28
Y	20.9	20.7	20.0	20.6	20.6	0.4	21.5	19.9
La(n)	33.4		32.2	34.7	32.3	1.7	34.7	28.4
Yb(n)	10.2		9.9	10.4	10.1	0.2	10.4	9.7
100Nb/Ti	0.10	0.11	0.09	0.10	0.10	0.01	0.12	0.09
Hf/Ta	4.74		4.30	4.43	4.72	0.46	5.73	4.30
Th/Hf	0.80		0.91	0.90	0.86	0.04	0.91	0.79
La(n)/Yb(n)	3.27		3.24	3.35	3.21	0.13	3.35	2.92
				contact				

MI = 100*(Fe2O3*/(Fe2O3* + MgO))

* total iron expressed as Fe2O3; n.a. : not analyzed

(n) : normalized to chondritic abundances (Anders and Ebihara, 1982)

Table 4: (continued)

Preakness Basalt

Sample:	PT-17-119.5	PT-17-127	PT-17-155	PT-17-166	PT-17-173	PT-17-222	PT-18-71	PT-18-83	PT-18-121	PT-18-133	PT-18-147	PT-18-161.5	PT-18-170
SiO2	51.57	50.73	52.31	52.36	51.07	51.56	52.70	50.78	51.51	51.42	51.13	51.55	50.28
TiO2	0.80	0.76	0.77	0.77	0.73	0.78	0.82	0.78	0.81	0.83	0.76	0.79	0.80
Al2O3	15.36	15.03	15.57	15.43	14.84	15.26	15.21	14.86	15.12	14.93	15.01	15.04	14.70
Fe2O3*	11.41	11.20	11.55	11.61	11.12	11.67	11.73	11.53	11.52	11.55	11.51	11.57	11.66
MnO	0.19	0.22	0.19	0.19	0.17	0.19	0.19	0.19	0.19	0.19	0.19	0.19	0.19
MgO	8.18	8.22	7.73	7.86	7.59	7.74	8.03	7.56	7.65	7.66	7.63	7.68	7.63
CaO	10.07	7.66	8.15	7.15	10.46	8.12	5.71	11.07	11.02	11.03	10.90	11.10	11.12
Na2O	2.44	4.71	4.21	4.88	4.01	4.64	5.14	1.99	2.16	2.13	2.03	2.03	2.04
K2O	0.38	0.66	0.13	0.11	0.07	0.07	0.19	0.19	0.21	0.19	0.21	0.17	0.17
P2O5	0.10	0.09	0.10	0.09	0.09	0.09	0.10	0.09	0.09	0.09	0.09	0.09	0.09
Total	100.50	99.28	100.71	100.45	100.15	100.12	99.82	99.04	100.28	100.02	99.46	100.21	98.68
analyses:	2	1	2	2	1	2	1	1	1	1	2	1	1
MI	58.2	57.7	59.9	59.6	59.4	60.1	59.4	60.4	60.1	60.1	60.1	60.1	60.4
Rb	6	14	2	2	1	1	4	11	12	10	10	7	9
Ba	108	214	78	78	32	53	62	71	66	63	76	93	87
Sr	132	119	423	308	61	209	149	133	127	126	127	132	133
Pb	7	4	5	4	3	4	4	5	3	4	3	4	2
Th	1			1		1	1	1	1	1	1	1	1
Zr	64	58	60	60	48	63	62	64	61	62	62	62	61
Hf	1.7			1.5		1.5	1.6	1.4	1.6	1.6	1.6	1.6	1.5
Nb	3.5	3.1	3.2	2.7	2.6	3.2	3.6	3.7	3.5	3.7	2.9	3.0	3.1
Ta	0.22			0.26		0.31	0.29	0.26	0.26	0.24	0.26	0.24	0.27
Ni	70	70	73	76	70	72	66	71	73	71	72	71	70
Zn	85	74	88	87	117	90	62	85	86	87	87	82	82
Cr	174	191	208	217	212	208	200	211	222	220	221	215	211
Ga	16	15	15	14	17	16	14	17	16	17	17	17	18
V	237	215	239	236	218	240	235	232	235	232	239	236	235
La	6.7			5.9		6.0	6.0	6.2	6.1	6.1	6.0	6.0	6.1
Ce	13.4			12.5		13.0	13.3	13.1	12.8	12.8	12.9	12.9	13.2
Nd	8.1			7.2		7.3	7.3	6.4	6.3	6.3	6.6	6.3	5.7
Sm	2.3			2.3		2.2	2.2	2.3	2.2	2.2	2.2	2.3	2.3
Eu	0.8			0.8		0.8	0.8	0.8	0.8	0.8	0.7	0.7	0.8
Tb	0.54			0.55		0.52	0.56	0.51	0.52	0.52	0.51	0.54	0.53
Yb	2.4			2.4		2.3	2.4	2.3	2.4	2.4	2.3	2.5	2.4
Lu	0.33			0.35		0.35	0.36	0.35	0.34	0.34	0.36	0.35	0.35
Y	20.4	19.4	20.2	20.5	18.6	20.6	20.7	20.7	19.9	20.2	19.9	20.3	19.9
La(n)	21.8			19.1		19.5	19.4	20.0	19.8	20.1	19.4	19.3	19.8
Yb(n)	11.7			11.7		11.0	11.3	11.2	11.6	11.7	11.2	11.8	11.3
100Nb/Ti	0.07	0.07	0.07	0.06	0.06	0.07	0.07	0.08	0.07	0.07	0.06	0.06	0.06
Hf/Ta	7.59			5.77		4.87	5.48	5.46	6.04	6.67	6.12	6.79	5.67
Th/Hf	0.85			0.85		0.93	0.84	0.94	0.87	0.88	0.86	0.82	0.85
La(n)/Yb(n)	1.86			1.64		1.77	1.72	1.78	1.71	1.72	1.74	1.63	1.76

MI = 100*(Fe2O3*/(Fe2O3* + MgO))

* total iron expressed as Fe2O3; n.a. : not analyzed

(n) : normalized to chondritic abundances (Anders and Ebihara, 1982)

Table 4: (continued)
Preakness Basalt

Sample:	PT-19-29	PT-19-56.5	PT-19-71.5	PT-19-107.5	PT-19-128	PT-19-206.5	PT-19-227	PT-19-235	PT-20-44	PT-20-60	PT-20-79	PT-20-108	PT-20-112.5
SiO2	52.53	52.53	52.31	52.33	52.75	52.13	52.81	52.64	53.86	52.86	54.31	53.64	**52.82**
TiO2	1.16	0.93	1.04	1.01	1.09	1.01	1.03	1.08	1.19	1.19	1.47	1.68	**1.28**
Al2O3	13.59	14.33	14.03	13.92	13.95	13.75	13.85	13.98	13.38	13.38	12.40	12.01	**14.05**
Fe2O3*	13.83	12.74	13.23	13.20	13.19	13.25	13.54	13.64	13.98	13.84	15.89	17.56	**14.60**
MnO	0.21	0.20	0.22	0.21	0.22	0.23	0.22	0.22	0.23	0.23	0.26	0.26	**0.21**
MgO	5.99	6.55	6.31	6.04	6.04	5.34	5.46	5.51	4.77	4.41	4.00	3.65	**3.85**
CaO	7.30	9.97	8.38	8.99	10.05	8.67	8.46	8.89	9.26	9.67	8.04	6.40	**9.70**
Na2O	4.85	2.76	3.65	3.56	2.49	3.17	3.70	3.39	2.59	2.62	3.14	3.67	**2.61**
K2O	0.46	0.31	0.88	0.95	0.62	1.67	0.83	0.78	0.76	0.77	0.86	0.92	**0.65**
P2O5	0.14	0.13	0.14	0.13	0.14	0.13	0.12	0.13	0.14	0.14	0.18	0.22	**0.15**
Total	100.06	100.45	100.19	100.34	100.54	99.35	100.02	100.26	100.16	99.11	100.55	100.01	**99.92**
analyses:	2	2	1	2	1	2	2	2	2	1	2	1	**2**
MI	69.8	66.0	67.7	68.6	68.6	71.3	71.3	71.2	74.6	75.8	79.9	82.8	**79.1**
Rb	15	6	29	33	20	54	30	23	26	26	26	26	**21**
Ba	67		143		143			186	181	192	205	253	**163**
Sr	96	133	135	135	132	221	175	134	140	140	139	104	**146**
Pb	5	8	4	5	6	7	4	4	8	7	6	4	**7**
Th	2	2	2		2	2		2	3		3	4	**3**
Zr	91	82	84	85	88	88	87	92	102	72	119	132	**105**
Hf	2.4	2.1	2.3		2.4	2.1		2.3	2.7		3.2	3.5	**2.8**
Nb	5.2	4.3	5.6	4.2	4.7	3.9	4.4	4.3	4.8	5.3	5.3	6.8	**4.4**
Ta	0.40	0.40	0.36		0.40	0.33		0.34	0.48		0.50	0.52	**0.41**
Ni	43	60	51	52	52	46	41	39	34	23	29	23	**26**
Zn	105	88	99	102	99	110	102	103	93	91	81	120	**84**
Cr	39	93	75	74	81	31	27	29	23	23	9	3	**11**
Ga	19	19	18	19	19	18	19	20	20	20	20	22	**21**
V	317	295	296	266	294	323	310	308	382	354	393	376	**326**
La	10.0	8.8	9.6		10.1	8.6		9.6	12.0		13.9	15.2	**11.7**
Ce	20.9	18.9	20.3		20.8	17.9		20.1	24.6		29.6	31.6	**24.2**
Nd	10.9	10.5	11.4		9.9	10.1		11.4	12.1		16.1	14.6	**11.5**
Sm	3.2	2.9	3.0		3.2	3.0		3.2	3.6		4.3	4.8	**3.8**
Eu	1.0	0.9	1.0		1.0	1.0		1.1	1.2		1.3	1.4	**1.2**
Tb	0.71	0.65	0.65		0.66	0.68		0.69	0.89		0.87	1.08	**0.80**
Yb	3.1	2.7	3.0		3.1	3.0		3.1	3.4		3.8	4.5	**3.6**
Lu	0.46	0.40	0.44		0.44	0.44		0.47	0.48		0.57	0.66	**0.52**
Y	26.9	24.4	25.1	25.3	25.9	26.8	27.0	27.2	27.7	27.2	32.6	38.4	**30.0**
La(n)	32.2	28.4	31.2		32.7	27.7		31.0	38.7		45.0	49.3	**38.0**
Yb(n)	15.0	12.9	14.6		14.7	14.5		15.1	16.2		18.2	21.8	**17.4**
100Nb/Tl	0.07	0.08	0.09	0.07	0.07	0.06	0.07	0.07	0.07	0.07	0.06	0.07	**0.06**
Hf/Ta	5.90	5.30	6.33		5.90	6.48		6.88	5.63		6.32	6.81	**6.76**
Th/Hf	0.97	0.98	0.92		0.96	1.02		0.93	1.15		1.09	1.00	**0.97**
La(n)/Yb(n)	2.15	2.21	2.14		2.23	1.92		2.05	2.39		2.48	2.27	**2.18**
											gabbroid	gabbroid	

MI = 100*(Fe2O3*/(Fe2O3* + MgO))
* total iron expressed as Fe2O3; n.a. : not analyzed
(n) : normalized to chondritic abundances (Anders and Ebihara, 1982)

Table 4: (continued)
Preakness Basalt

Sample:	PT-20-120	PT-20-145	PT-20-197	PT-20-227	PT-20-278	PTI-3-4	PTI-3-40	PTI-3-117	Average	Std Dev	Maximum	Minimum
SiO2	54.10	53.31	53.33	53.03	53.04	52.96	53.13	49.26	52.31	1.12	54.31	49.26
TiO2	2.21	1.12	0.96	0.94	0.87	1.05	1.06	1.08	1.02	0.30	2.21	0.73
Al2O3	11.03	14.55	12.52	13.01	13.63	14.15	13.98	14.40	14.13	1.05	15.57	11.03
Fe2O3*	19.16	13.84	13.51	13.58	13.01	13.60	13.72	12.79	13.10	1.78	19.16	11.12
MnO	0.27	0.21	0.23	0.23	0.23	0.22	0.22	0.20	0.21	0.02	0.27	0.17
MgO	2.45	4.22	6.86	6.97	6.95	5.55	5.51	5.55	6.27	1.54	8.22	2.45
CaO	6.47	8.89	10.13	10.14	9.88	9.87	9.86	12.65	9.27	1.58	12.65	5.71
Na2O	3.00	3.35	2.16	2.14	2.58	2.65	2.52	3.29	3.13	0.95	5.14	1.99
K2O	1.12	0.75	0.54	0.50	0.65	0.62	0.59	0.90	0.56	0.36	1.67	0.07
P2O5	0.27	0.14	0.11	0.11	0.10	0.12	0.13	0.16	0.12	0.04	0.27	0.09
Total	100.08	100.38	100.35	100.65	100.94	100.79	100.72	100.28	100.11			
analyses:	2	1	2	2	2	2	1	2	samples	34		
MI	88.7	76.6	66.3	66.1	65.2	71.0	71.3	69.7	67.6	7.9	88.7	57.7
Rb	32	29	18	16	21	20	18	16	17	12	54	1
Ba	372		138	140	157	144	154	141	133	73	372	32
Sr	103	159	130	130	130	139	141	155	150	63	423	61
Pb	6	6	5	7	5	9	7	6	5	2	9	2
Th	5			2	2		2	2	2	1	5	1
Zr	175	98	81	78	73	90	91	87	82	25	175	48
Hf	4.7			2.0	2.0		2.3	2.3	2.2	0.8	4.7	1.4
Nb	9.1	4.7	4.2	3.2	3.8	4.1	3.7	4.5	4.2	1.3	9.1	2.6
Ta	0.72			0.31	0.32		0.40	0.30	0.35	0.11	0.72	0.22
Ni	20	16	40	43	34	30	32	31	50	19	76	16
Zn	183	88	89	90	90	99	102	132	96	20	183	62
Cr	5	9	38	42	45	32	34	26	102	88	222	3
Ga	22	21	18	19	18	20	20	18	18	2	22	14
V	406	286	343	341	306	314	318	321	291	55	406	215
La	18.6			8.4	7.7		9.4	8.9	8.9	3.3	18.6	5.9
Ce	40.3			17.5	17.1		19.6	19.0	18.9	7.0	40.3	12.5
Nd	20.2			8.1	8.4		10.4	11.3	9.8	3.5	20.2	5.7
Sm	6.1			2.7	2.6		3.2	3.1	3.0	0.9	6.1	2.2
Eu	1.6			0.9	0.9		1.0	1.0	1.0	0.2	1.6	0.7
Tb	1.30			0.63	0.68		0.74	0.73	0.68	0.19	1.30	0.51
Yb	5.7			2.7	2.7		3.2	3.0	3.0	0.8	5.7	2.3
Lu	0.81			0.42	0.40	1.80	0.49	0.44	0.49	0.29	1.80	0.33
Y	48.5	28.5	25.1	24.4	22.2	27.4	27.8	27.0	25.2	6.0	48.5	18.6
La(n)	60.3			27.1	24.7		30.5	28.7	29.0	10.7	60.3	19.1
Yb(n)	27.6			13.0	12.8		15.6	14.5	14.3	3.8	27.6	11.0
100Nb/Ti	0.07	0.07	0.07	0.06	0.07	0.07	0.06	0.07	0.07	0.01	0.09	0.06
Hf/Ta	6.58			6.58	6.19		5.68	7.80	6.22	0.69	7.80	4.87
Th/Hf	1.00			0.94	0.92		0.99	0.93	0.94	0.08	1.15	0.82
La(n)/Yb(n)	2.19			2.09	1.94		1.96	1.98	1.98	0.24	2.48	1.63
	gabbroid											

MI = 100*(Fe2O3*/(Fe2O3* + MgO))
* total iron expressed as Fe2O3; n.a. : not analyzed
(n) : normalized to chondritic abundances (Anders and Ebihara, 1982)

Table 4: (continued)
Hook Mountain Basalt

Sample:	PT-10-169.5	PT-10-180	PT-10-195	PT-10-201	PT-11-23	PT-11-42	PT-11-61	PT-11-68.5	PT-11-72.5	PT-11-84.5
SiO2	48.90	50.85	50.07	50.19	49.77	50.32	50.40	50.21	50.40	50.47
TiO2	1.31	1.35	1.33	1.35	1.37	1.33	2.24	1.33	1.36	1.32
Al2O3	13.20	13.69	13.48	13.52	13.65	13.51	11.07	13.82	13.12	13.44
Fe2O3*	14.25	15.75	15.66	15.83	15.66	15.59	18.59	15.76	16.18	16.03
MnO	0.24	0.22	0.24	0.23	0.23	0.23	0.25	0.23	0.25	0.24
MgO	5.68	6.11	5.92	5.87	5.51	5.67	2.64	5.71	5.55	5.96
CaO	9.05	7.02	8.05	8.79	11.07	8.02	8.63	9.39	9.83	10.2
Na2O	4.22	4.73	4.22	3.76	2.40	4.17	5.42	2.77	2.98	2.29
K2O	0.51	0.47	0.59	0.65	0.52	0.71	0.15	0.59	0.67	0.46
P2O5	0.15	0.16	0.15	0.15	0.16	0.15	0.42	0.14	0.13	0.15
Total	97.52	100.35	99.71	100.34	100.34	99.70	99.81	99.95	100.47	100.56
analyses:	3	2	1	2	2	2	2	1	2	1
MI	71.5	72.0	72.6	72.9	74.0	73.3	87.6	73.4	74.5	72.9
Rb	10	8	13	17	14	18	4	16	19	16
Ba	115	180	110	154	116	94	98	115	108	
Sr	131	137	91	162	103	111	30	97	97	105
Pb	2	5	7	7	7	3	6	5	6	5
Th			2	2		2	5	2	2	2
Zr	97	100	92	93	105	95	92	90	85	97
Hf			2.4	2.6		2.6	7.0	2.5	2.2	2.8
Nb	4.2	3.7	4.5	3.2	4.3	4.2	4.5	4.2	2.6	3.9
Ta			0.30	0.35		0.27	0.87	0.37	0.30	0.30
Ni	68	72	66	69	76	27	68	67	63	71
Zn	97	95	104	83	116	81	82	83	99	106
Cr	68	67	71	66	69	1	71	69	66	71
Ga	18	20	18	18	20	18	27	20	18	20
V	339	357	367	328	357	173	336	351	422	354
La			7.8	8.1		7.5	20.6	7.5	7.1	8.4
Ce			16.9	17.1		16.7	46.0	16.8	15.1	18.7
Nd			8.1	10.6		8.7	24.9	9.9	9.0	10.9
Sm			3.3	3.5		3.4	9.1	3.4	3.0	3.7
Eu			1.1	1.1		1.1	2.3	1.1	1.1	1.2
Tb			0.80	0.97		0.82	2.18	0.79	0.77	0.94
Yb			3.7	3.9		3.6	9.2	3.7	3.6	4.0
Lu			0.53	0.56		0.54	1.31	0.55	0.51	0.58
Y	33.3	34.2	33.0	34.3	35.1	32.9	84.4	32.3	30.3	35.0
La(n)			25.2	26.1		24.4	66.6	24.2	22.9	27.3
Yb(n)			17.8	18.5		17.4	44.1	17.7	17.4	19.2
100Nb/Ti		0.05	0.06	0.04	0.05		0.03	0.05	0.03	0.05
Hf/Ta			8.13	7.43		9.52	7.99	6.68	7.43	9.33
Th/Hf			0.77	0.72		0.72	0.75	0.70	0.72	0.73
La(n)/Yb(n)			1.41	1.41		1.40	1.51	1.36	1.32	1.42
							gabbroid			

MI = 100*(Fe2O3*/(Fe2O3* + MgO))
* total iron expressed as Fe2O3; n.a. : not analyzed
(n) : normalized to chondritic abundances (Anders and Ebihara, 1982)

Table 4: (continued)
Hook Mountain Basalt

Sample:	PT-11-108	PT-11-131	PT-11-138.5	PT-11-154	PT-11-195	PT-11-203	PT-11-215	PT-11-235	PT-11-239	PT-11-254
SiO2	50.15	50.77	51.08	50.92	50.58	49.90	50.96	50.73	50.00	47.37
TiO2	1.33	1.35	1.38	1.41	1.45	1.44	1.42	1.40	1.41	1.82
Al2O3	13.35	13.39	13.41	13.43	13.71	13.46	13.38	13.31	13.45	17.25
Fe2O3*	16.01	16.15	16.22	16.31	16.54	16.49	16.35	16.23	16.56	14.32
MnO	0.24	0.24	0.24	0.24	0.25	0.24	0.24	0.24	0.29	0.19
MgO	5.93	5.89	5.67	5.56	5.82	5.63	5.58	5.55	5.73	4.40
CaO	10.25	10.15	10.00	10.05	7.05	10.73	10.06	10.03	10.23	10.04
Na2O	2.15	2.33	2.39	2.34	3.69	2.32	2.48	2.34	2.35	3.41
K2O	0.44	0.49	0.53	0.54	1.26	0.21	0.25	0.44	0.34	0.55
P2O5	0.15	0.16	0.17	0.18	0.18	0.18	0.19	0.19	0.18	0.24
Total	100.00	100.92	101.09	100.98	100.53	100.60	100.91	100.46	100.54	99.59
analyses:	2	2	2	1	2	1	2	2	2	1
MI	73.0	73.3	74.1	74.6	74.0	74.5	74.6	74.5	74.3	76.5
Rb	15	15	20	20	30	4	14	12	7	9
Ba	116							148	142	138
Sr	103	109	107	109	150	114	112	120	124	212
Pb	6	7	6	6	7	8	8	8	6	4
Th			2		2		2		2	
Zr	96	100	101	108	112	114	113	111	111	133
Hf			2.9		2.9		2.9		2.9	
Nb	3.6	3.6	3.8	4.0	5.0	4.9	5.1	5.0	4.9	5.8
Ta			0.37		0.38		0.36		0.36	
Ni	71	64	69	63	57	60	57	51	51	82
Zn	107	112	115	117	149	143	149	118	119	454
Cr	70	64	62	61	64	63	67	62	57	91
Ga	19	21	21	20	17	18	20	20	21	23
V	339	339	350	328	370	364	354	328	334	482
La			9.1		9.4		10.0		10.0	
Ce			19.7		21.1		20.8		21.3	
Nd			10.9		12.9		12.4		11.6	
Sm			3.8		4.0		4.0		4.0	
Eu			1.2		1.3		1.3		1.3	
Tb			0.99		1.00		0.96		0.98	
Yb			4.3		4.3		4.4		4.4	
Lu			0.61		0.63		0.62		0.63	
Y	33.9	35.4	36.2	37.2	37.7	37.7	38.1	37.2	38.0	47.6
La(n)			29.3		30.4		32.3		32.2	
Yb(n)			20.7		20.8		21.3		21.1	
100Nb/Ti	0.05	0.04	0.05	0.05	0.06	0.06	0.06	0.06	0.06	0.05
Hf/Ta			7.86		7.71		8.00		8.08	
Th/Hf			0.79		0.76		0.85		0.86	
La(n)/Yb(n)			1.42		1.46		1.52		1.53	
										contact

MI = 100*(Fe2O3*/(Fe2O3* + MgO))
* total iron expressed as Fe2O3; n.a. : not analyzed
(n) : normalized to chondritic abundances (Anders and Ebihara, 1982)

Table 4: (continued)
Hook Mountain Basalt

Sample:	Average	Std Dev	Maximum	Minimum
SiO2	50.27	0.80	51.08	47.37
TiO2	1.44	0.22	2.24	1.32
Al2O3	13.55	1.06	17.25	11.07
Fe2O3*	16.12	0.78	18.59	14.32
MnO	0.24	0.02	0.29	0.19
MgO	5.51	0.78	6.11	2.64
CaO	9.45	1.18	11.07	7.02
Na2O	3.08	0.98	5.42	2.15
K2O	0.52	0.23	1.26	0.15
P2O5	0.18	0.06	0.42	0.13
Total	100.36			
analyses:	samples	20		
MI	74.6	3.3	87.6	72.0
Rb	14	6	30	4
Ba	126	25	180	94
Sr	116	35	212	30
Pb	6	1	8	2
Th	2	1	5	2
Zr	102	11	133	85
Hf	3.1	1.3	7.0	2.2
Nb	4.3	0.7	5.8	2.6
Ta	0.38	0.17	0.87	0.27
Ni	64	12	82	27
Zn	126	80	454	81
Cr	64	16	91	1
Ga	20	2	27	17
V	349	55	482	173
La	9.6	3.8	20.6	7.1
Ce	20.9	8.6	46.0	15.1
Nd	11.8	4.6	24.9	8.1
Sm	4.1	1.7	9.1	3.0
Eu	1.3	0.3	2.3	1.1
Tb	1.02	0.40	2.18	0.77
Yb	4.5	1.6	9.2	3.6
Lu	0.64	0.23	1.31	0.51
Y	38.2	11.4	84.4	30.3
La(n)	31.0	12.3	66.6	22.9
Yb(n)	21.5	7.7	44.1	17.4
100Nb/Ti	0.05	0.01	0.06	0.03
Hf/Ta	8.02	0.81	9.52	6.68
Th/Hf	0.76	0.05	0.86	0.70
La(n)/Yb(n)	1.43	0.07	1.53	1.32

MI = 100*(Fe2O3*/(Fe2O3* + MgO))
* total iron expressed as Fe2O3; n.a. : not analyzed
(n) : normalized to chondritic abundances (Anders and Ebihara, 1982)